

Point-source radiation in attenuative anisotropic media

Bharath Shekar & Ilya Tsvankin

Center for Wave Phenomena, Colorado School of Mines, Golden CO 80401

ABSTRACT

Important insights into point-source radiation in attenuative anisotropic media can be gained by applying asymptotic methods. Here, we derive the asymptotic Green's function in homogeneous, attenuative, arbitrarily anisotropic media using the steepest-descent method. The saddle-point condition helps describe the behavior of the slowness and group-velocity vectors of the P-, S_1 -, and S_2 -waves in the far field. We test the accuracy of the asymptotic analysis by comparing it with the ray-perturbation method for P-waves in transversely isotropic media.

Key words: attenuation, anisotropy, asymptotic analysis, inhomogeneity angle

Introduction

Velocity and attenuation anisotropy significantly influence the radiation pattern of seismic waves excited by a point source. A proper correction for the source directivity can help improve the robustness of AVO (amplitude variation with offset) and attenuation analysis. Point-source radiation in homogeneous anisotropic media has been mostly studied for nonattenuative materials using both asymptotic and numerical methods (e.g. Červený, 2001; Tsvankin, 2012; Gajewski 1993; Wang and Achenbach, 1994). Zhu (2006) presents an analytic and numerical study of point-source radiation in 2D homogeneous attenuative TI media. Vavryčuk (2007) derives the asymptotic Green's function for arbitrarily anisotropic, homogeneous, attenuative models by formally extending the results of Wang and Achenbach (1994).

In attenuative media, the Christoffel matrix becomes complex-valued because the stiffness tensor is complex. Although many results derived for elastic media can be generalized for attenuative media, there are several important differences. In asymptotic analysis for attenuative media, the saddle-point condition involves complex-valued slowness and group-velocity vectors, whose properties have to be clearly defined. Also, the expression for the eigenvalue of the complex Christoffel matrix in Vavryčuk (2007) is inaccurate, which distorts the analytic expression for the Green's function. Here, we present a rigorous derivation of the saddle-point condition and the eigenvalue of the complex Christoffel matrix.

We start by reviewing the definitions of the attenuation coefficient, group velocity, and other key signa-

tures in attenuative media. Then the integral expression for the Green's function in homogeneous attenuative anisotropic media is evaluated by the steepest-descent method. The saddle-point condition is used to study the properties of the far-field P-wave. Finally, we compare the P-wave group velocity, polarization, and slowness vectors obtained from our asymptotic analysis for VTI (transversely isotropic with a vertical symmetry axis) media with those found from ray perturbation theory (Červený and Pšenčík, 2009).

Basic Definitions

In attenuative media, the wave vector is complex-valued (complex quantities are denoted by the tilde sign on top):

$$\begin{aligned}\tilde{\mathbf{k}} &= \mathbf{k}^R + i\mathbf{k}^I, \\ &= \omega(\mathbf{p}^R + i\mathbf{p}^I),\end{aligned}\tag{1}$$

where \mathbf{p}^R and \mathbf{p}^I are the real-valued propagation and attenuation vectors, respectively, which form the slowness vector $\tilde{\mathbf{p}} = \mathbf{p}^R + i\mathbf{p}^I$. The orientations of \mathbf{k}^R and \mathbf{k}^I (or equivalently, of \mathbf{p}^R and \mathbf{p}^I) can be different, and the angle between \mathbf{k}^R and \mathbf{k}^I is called the “inhomogeneity angle” ξ (Červený et al., 2008; Behura and Tsvankin, 2009; Tsvankin and Grechka, 2011). Plane waves satisfy the wave equation with arbitrary values of ξ , except for certain “forbidden directions” of \mathbf{p}^I (Krebes and Le, 1994; Červený and Pšenčík, 2005; Carcione, 2007). Hence, the angle ξ is treated as a free parameter in plane-wave propagation (Behura and Tsvankin, 2009).

However, for waves excited by point-sources, the inhomogeneity angle is determined by medium properties and boundary conditions (Vavryčuk, 2007; Zhu, 2006). In reflection/transmission problems for plane waves, the inhomogeneity angle is constrained by Snell's law (Hearn and Krebs, 1990; Behura and Tsvankin, 2009).

Zhu and Tsvankin (2006) define the phase attenuation coefficient \mathcal{A} as

$$\mathcal{A} = \frac{|\mathbf{k}^I|}{|\mathbf{k}^R|}. \quad (2)$$

The angle-dependent quality factor Q is given by

$$Q = \frac{1}{2\mathcal{A}}. \quad (3)$$

Červený and Pšenčík (2008) show that the group attenuation coefficient responsible for attenuation-related amplitude decay along seismic rays can be written as:

$$\mathcal{A}^{\text{gr}} = \frac{\mathbf{p}^I \cdot \mathbf{F}^R}{\mathbf{p}^R \cdot \mathbf{F}^R}, \quad (4)$$

where \mathbf{F}^R denotes the real part of the Poynting vector. The complex-valued Poynting vector characterizes the direction of energy flux, and its real part coincides with the group velocity vector:

$$F_i^R = \kappa \text{Re}[\tilde{a}_{ijkl} \tilde{p}_l \tilde{g}_j^* \tilde{g}_i], \quad (5)$$

where κ is a constant, \tilde{a}_{ijkl} are the complex-valued density-normalized stiffness coefficients, and \tilde{g}_j are the components of the complex-valued polarization vector $\tilde{\mathbf{g}}$ that satisfies $\tilde{\mathbf{g}}^* \cdot \tilde{\mathbf{g}} = 1$; the asterisk “*” denotes the complex conjugate. Behura and Tsvankin (2009) prove that the group attenuation coefficient is practically independent of the inhomogeneity angle and coincides with the phase attenuation coefficient for $\xi = 0$, except for the vicinity of the forbidden directions. Similar results follow from the perturbation analysis presented by Červený and Pšenčík (2009).

Asymptotic Green's function in homogeneous attenuative anisotropic media

Here, we derive the asymptotic Green's function for P- and S-waves in a homogeneous, attenuative, arbitrarily anisotropic medium. The analysis is valid for all three wave modes (P, S_1 , S_2), but breaks down in the vicinity of shear-wave singularities where the Christoffel equation has degenerate (coincident) eigenvalues.

The exact Green's function can be found from the wave equation as (Appendix A, equation 30):

$$G_{kn}(\mathbf{x}, \mathbf{x}^0, \omega) = \frac{i\omega}{(2\pi)^2} \int_{-\infty}^{\infty} \int_{-\infty}^{\infty} \left[\frac{\tilde{S}_{kn}}{\partial[\det(\tilde{\Gamma} - \mathbf{I})]/\partial p_3} \right]_{p_3 = \tilde{p}_3^r} \times e^{-\omega R \tilde{\phi}} dp_1 dp_2, \quad (6)$$

where

$$\tilde{\phi} = -i(p_1 \hat{x}_1 + p_2 \hat{x}_2 + \tilde{p}_3^r \hat{x}_3), \quad (7)$$

$R = \sqrt{[(x_1 - x_1^0)^2 + (x_2 - x_2^0)^2 + (x_3 - x_3^0)^2]}$ is the source-receiver distance, \hat{x}_i is the unit vector in the source-receiver direction, p_j are the slowness components, $\tilde{\Gamma}_{ik} = \tilde{a}_{ijkl} p_j p_l$, and S_{kn} are the cofactors of the matrix $\tilde{\Gamma} - \mathbf{I}$, \mathbf{I} is the identity matrix. The solution of the equation $\det[\tilde{a}_{ijkl} p_j p_l - \delta_{ik}] = 0$ is denoted as $\tilde{p}_3^r = \tilde{p}_3(p_1, p_2)$.

The components of the slowness vector satisfy the following equation:

$$\det[\tilde{a}_{ijkl} p_j p_l - G \delta_{ik}] = 0, \quad (8)$$

where

$$G(p_i, x_i) = 1 \quad (9)$$

is the eigenvalue of the matrix $\tilde{\Gamma}_{ik} = \tilde{a}_{ijkl} p_j p_l$. Equations 8 or 9 represent the eikonal equation in anisotropic media (Červený, 2001). The eigenvector \tilde{U}_i corresponding to the eigenvalue G is the polarization vector that satisfies the following equation:

$$\tilde{\Gamma}_{ik} \tilde{U}_k = G \tilde{U}_i. \quad (10)$$

If we assume that $\omega R/v$ (where v is a certain average of the group velocity) is a large parameter, G_{kn} (equation 6) can be evaluated by steepest-descent integration near the saddle point (Bleistein, 1984). The saddle-point condition is

$$\frac{\partial \tilde{\phi}}{\partial p_1} = \frac{\partial \tilde{\phi}}{\partial p_2} = 0, \quad (11)$$

i.e.,

$$\begin{aligned} \hat{x}_1 + \hat{x}_3 \left[\frac{\partial \tilde{p}_3(p_1, p_2)}{\partial p_1} \right]_{\tilde{p}_1^s, \tilde{p}_2^s} &= 0, \\ \hat{x}_2 + \hat{x}_3 \left[\frac{\partial \tilde{p}_3(p_1, p_2)}{\partial p_2} \right]_{\tilde{p}_1^s, \tilde{p}_2^s} &= 0, \end{aligned} \quad (12)$$

where $(\tilde{p}_1^s, \tilde{p}_2^s)$ denotes the saddle point. The partial derivatives in equation 12 can be calculated from the function G (equation 9) using the implicit function theorem (Courant, 1988). Then equation 12 becomes:

$$\begin{aligned} \hat{x}_1 \left[\frac{\partial G}{\partial p_3} \right]_{\tilde{p}_1^s, \tilde{p}_2^s} - \hat{x}_3 \left[\frac{\partial G}{\partial p_1} \right]_{\tilde{p}_1^s, \tilde{p}_2^s} &= 0, \\ \hat{x}_2 \left[\frac{\partial G}{\partial p_3} \right]_{\tilde{p}_1^s, \tilde{p}_2^s} - \hat{x}_3 \left[\frac{\partial G}{\partial p_2} \right]_{\tilde{p}_1^s, \tilde{p}_2^s} &= 0; \end{aligned} \quad (13)$$

$$\frac{\partial G}{\partial p_j} = \frac{\partial \tilde{\Gamma}_{ik}}{\partial p_j} \frac{\tilde{S}_{ik}}{\tilde{S}}. \quad (14)$$

The derivatives $\partial \tilde{\Gamma}_{ik}/\partial p_j$ and \tilde{S}_{ik}/\tilde{S} can be found by substituting the complex-valued stiffness tensor in the definitions of $\partial \Gamma_{ik}/\partial p_j$ and S_{jk}/S given in Červený (1972). Since G is a homogeneous function of second degree in p_j , Euler's homogeneous function theorem yields:

$$p_j \frac{\partial G}{\partial p_j} = 2. \quad (15)$$

Next, we introduce the vector $\tilde{\mathbf{E}}$ as

$$\tilde{E}_j = \frac{1}{2} \frac{\partial G}{\partial p_j}. \quad (16)$$

In elastic media, equation 16 defines the components of the group-velocity vector. In attenuative media, $\tilde{\mathbf{E}}$ has been termed “energy velocity” (Vavryčuk, 2007), with its real part contributing to the traveltime and the imaginary part to energy dissipation. Since the unit vector in the source-receiver direction $\hat{\mathbf{x}}$ is real-valued, equation 13 implies that at the saddle point the vector $\tilde{\mathbf{E}} = \tilde{\beta} \hat{\mathbf{x}}$, where $\tilde{\beta}$ is a complex constant. Hence, the real and imaginary parts of the energy-velocity vector are parallel to the vector connecting the source and the receiver (i.e., $\text{Re}[\tilde{\mathbf{E}}] \parallel \hat{\mathbf{x}}$ and $\text{Im}[\tilde{\mathbf{E}}] \parallel \hat{\mathbf{x}}$).

Evaluating the integral in equation 6 by the method of steepest descent (Bleistein, 2012), we find:

$$G_{kn}(\mathbf{x}, \mathbf{x}^0, \omega) = \frac{i}{(2\pi)} \frac{1}{\sqrt{\det \tilde{\mathbf{\Phi}}''}} \times \frac{\tilde{S}_{kn}}{\partial[\det(\tilde{\mathbf{\Gamma}} - \mathbf{I})]/\partial p_3} \exp(-\omega R \tilde{\phi}), \quad (17)$$

where all quantities are obtained at $(\tilde{p}_1^s, \tilde{p}_2^s, \tilde{p}_3^r)$, and $\tilde{\mathbf{\Phi}}''$ is the Hessian matrix of the partial derivatives of $\tilde{\phi}$ with respect to p_1 and p_2 . The matrix $\tilde{\mathbf{\Phi}}''$ can be computed from equation 8 using the implicit function theorem. The phase function at the saddle point can be found from equations 7, 13, and 15:

$$\tilde{\phi} = -\frac{i}{\sqrt{E_j^2}}. \quad (18)$$

In the next section, we show that the real part of E_j contributes to the traveltime and the imaginary part to attenuation. For 2D VTI media, equation 17 reduces to the expression for the Green’s function derived by Zhu (2006).

Although the asymptotic analysis carried out above is similar to that presented by Vavryčuk (2007), we proved (rather than assumed) that at the saddle point the real and imaginary parts of the “energy-velocity” vector are parallel to each other. To derive expressions for the “energy-velocity” vector and the Gaussian curvature of the slowness surface (which is related to the Hessian matrix obtained by the steepest-descent method), Vavryčuk (2007) uses the following expression for the eigenvalue G :

$$G = \tilde{a}_{ijkl} p_j p_l \tilde{U}_i \tilde{U}_k, \quad (19)$$

where \mathbf{U} is the polarization vector (equation 10). Equation 19, however, is not valid for complex symmetric matrices (Horn and Johnson, 1990). Instead, we employed the implicit function theorem to evaluate the “energy-velocity” vector and the Hessian matrix.

Model	1	2	3	4
V_{P0} (km/s)	3.00	3.00	3.00	3.00
V_{S0} (km/s)	1.50	1.50	1.50	1.50
ϵ	0.10	0.40	0.40	0.40
δ	0.005	0.25	0.25	0.25
Q_{P0}	100	100	10	100
Q_{S0}	60	60	10	10
ϵ_Q	-0.20	0.45	0	0
δ_Q	-0.10	-0.50	0	0

Table 1. Homogeneous TI models with anisotropic velocity and attenuation functions. The parameters V_{P0} and V_{S0} are the vertical P- and S-wave vertical velocities, Q_{P0} and Q_{S0} are the vertical P-wave and S-wave quality factors, and ϵ_Q and δ_Q are the attenuation-anisotropy parameters defined in Zhu and Tsvankin (2006).

Numerical Examples

In this section, the analytic results presented above are used to study the behavior of the inhomogeneity angle and the group-velocity and polarization vectors in homogeneous, attenuative VTI media. Table 1 shows the parameters of the velocity and attenuation functions for four VTI models defined in Zhu (2006).

First, we analyze the energy-velocity vector defined in equation 16. Červený et al. (2008) demonstrate that the perturbed group velocity $\tilde{\mathbf{U}}$ in attenuative media is given by

$$\tilde{U}_i = (1 - i\mathcal{A})\mathcal{U}_i, \quad (20)$$

where \mathcal{U} is the group-velocity vector in the reference elastic medium and \mathcal{A} is the phase attenuation coefficient computed for a zero inhomogeneity angle in the phase direction that corresponds to the given group direction. The complex-valued energy-velocity vector $\tilde{\mathbf{E}}$ is compared with the perturbed group velocity $\tilde{\mathbf{U}}$ in Figure 1. Both the real and imaginary parts of the vectors coincide, so our solution for $\tilde{\mathbf{E}}$ accurately describes both the traveltime and attenuation along the ray.

Equation 8 and the saddle-point condition (equation 13) can be used to compute the complex-valued slowness vector $\tilde{\mathbf{p}}$ and, hence, the corresponding inhomogeneity angle. For the purpose of numerical computations, it is convenient to parametrize $\tilde{\mathbf{p}}$ in the following way (Červený and Pšenčík, 2005):

$$\tilde{\mathbf{p}} = \tilde{\sigma} \mathbf{n} + i D \mathbf{m}, \quad (21)$$

where the vector \mathbf{n} specifies the phase direction and \mathbf{m} is chosen to be perpendicular to \mathbf{n} (i.e., $\mathbf{n} \cdot \mathbf{m} = 0$).

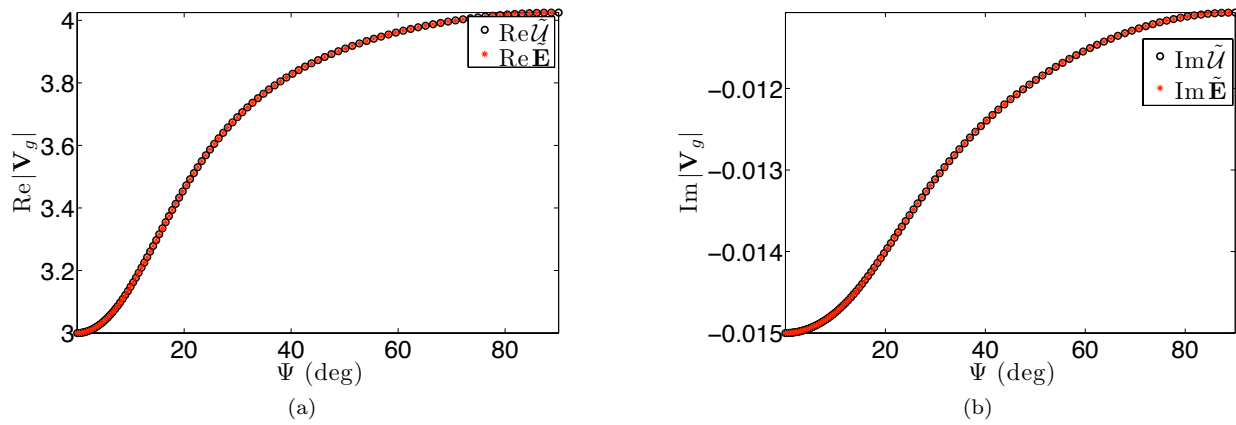


Figure 1. Comparison of the magnitudes of the energy-velocity vector $\tilde{\mathbf{E}}$ (equation 16) and perturbed P-wave group velocity vector $\tilde{\mathbf{U}}$ (equation 20) for model 2 from Table 1. The magnitudes of (a) real and (b) imaginary parts of $|\tilde{\mathbf{U}}|$ and $|\tilde{\mathbf{E}}|$; Ψ is the group angle with the vertical.

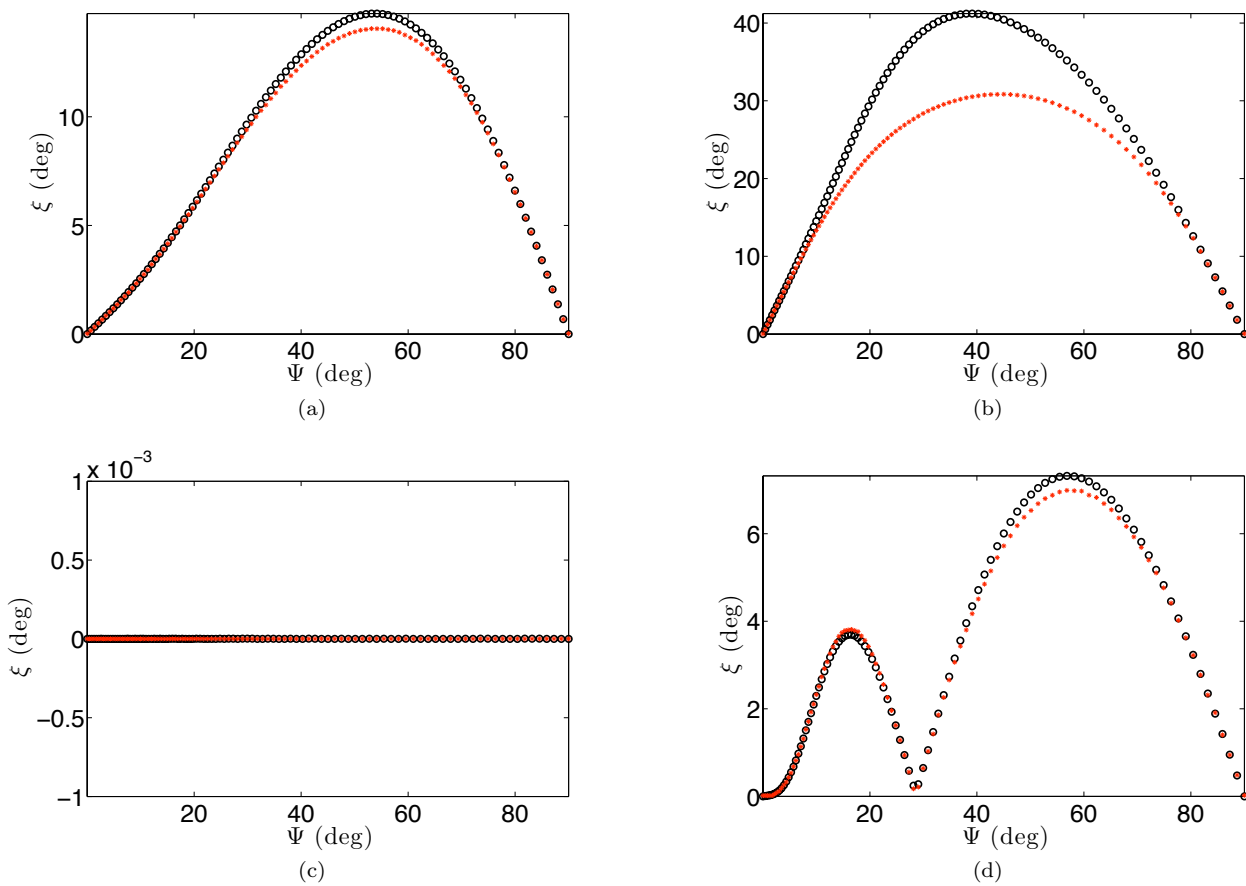


Figure 2. Inhomogeneity angle ξ computed from the asymptotic analysis in this paper (red stars) and ray perturbation theory (black circles) for models (a) 1, (b) 2, (c) 3, and (d) 4.

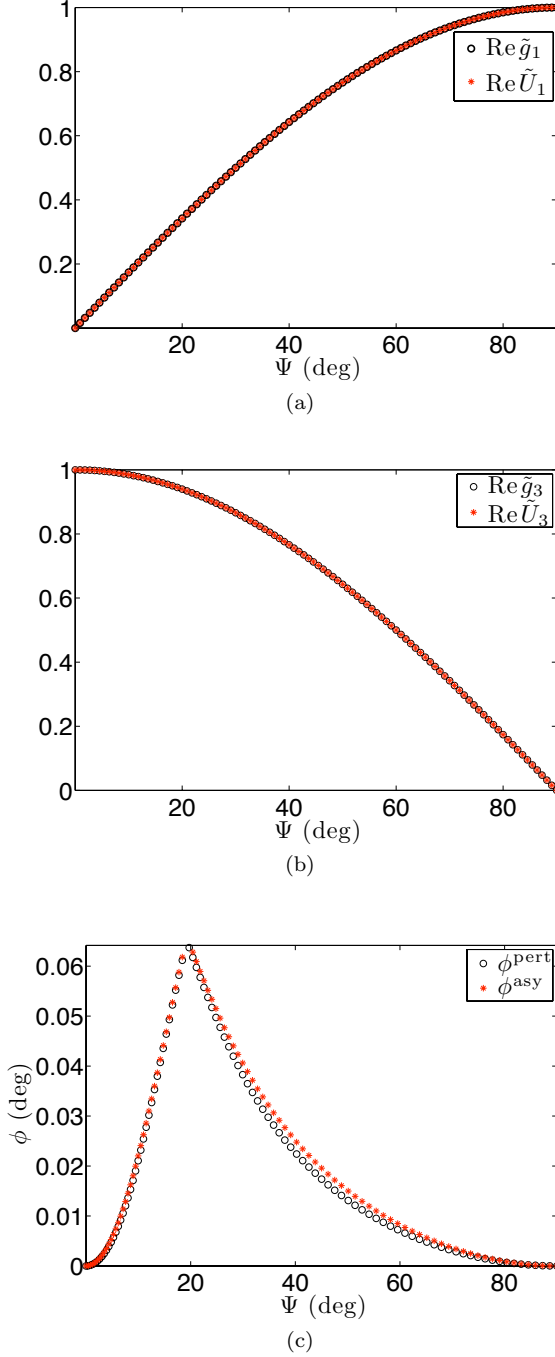


Figure 3. Comparison of the complex-valued polarization vectors $\tilde{\mathbf{U}}$ and $\tilde{\mathbf{g}}$ for model 2. The (a) X-component and (b) Z-component of the real parts of $\tilde{\mathbf{U}}$ and $\tilde{\mathbf{g}}$. (c) The phase of $\tilde{\mathbf{U}}$ (ϕ^{asym}) and $\tilde{\mathbf{g}}$ (ϕ^{pert}).

The quantity D is called the inhomogeneity parameter (Červený and Pšenčík, 2005). In our examples with VTI models, we can assume that \mathbf{n} is confined to the $[x_1, x_3]$ -plane, and we can choose \mathbf{m} to lie in the same plane. To find the parameters $\tilde{\sigma}$ and D corresponding to the saddle point, we solve the constrained optimization problem:

$$\text{Minimize } \left\| \frac{\tilde{\mathbf{E}}}{\sqrt{\tilde{E}_j^2}} - \hat{\mathbf{x}} \right\|_2^2, \quad \text{subject to } G = 1. \quad (22)$$

Therefore, the objective function is the difference between the orientation of $\tilde{\mathbf{E}}$ and $\hat{\mathbf{x}}$ (equation 13), with equation 8 serving as a constraint.

Figure 2 compares the inhomogeneity angle ξ computed from our asymptotic analysis and the ray-perturbation approach (see Appendix B, equation 10). The values of ξ obtained by the two methods are close to one another for models 1, 3, and 4. The discrepancy for model 2 can be expected because P-wave attenuation for that model is strongly anisotropic. Indeed, the perturbation method assumes the magnitude of attenuation and attenuation anisotropy to be small. Although model 3 has substantial attenuation and an anisotropic velocity function, the inhomogeneity angle for that model vanishes because the quality-factor components Q_{ij} are identical (see Appendix B).

The polarization vector $\tilde{\mathbf{U}}$ for the plane wave that corresponds to the saddle-point condition can be computed from equation 10. Using ray perturbation theory, an approximate polarization vector $\tilde{\mathbf{g}}$ can be obtained from equation 6. Figure 3 shows the real parts and phases of the complex-valued vectors $\tilde{\mathbf{U}}$ and $\tilde{\mathbf{g}}$ for model 2. While the real parts practically coincide, there is a small difference between the phase terms. Clearly, our analysis accurately describes the direction of the P-wave particle motion. The imaginary parts of $\tilde{\mathbf{U}}$ and $\tilde{\mathbf{g}}$ vanish for model 3 because the attenuation function is isotropic.

Conclusions

We presented a rigorous derivation of the Green's function in homogeneous, attenuative, arbitrarily anisotropic media using the steepest-descent method. Application of the saddle-point condition helps identify the plane wave that makes the most significant contribution to the displacement field of each mode. Our results make it possible to evaluate the inhomogeneity angle and describe the behavior of the group-velocity vector in the high-frequency approximation.

P-wave signatures obtained from our asymptotic analysis for TI media were compared with the same quantities computed by ray perturbation theory. The asymptotic energy-velocity vector is close to the perturbed group-velocity vector and, therefore, correctly predicts the traveltime and attenuation along the ray.

The inhomogeneity angles computed from the saddle-point condition and perturbation theory differ only for strongly attenuative models. The polarization vector is complex, and both the real and imaginary parts are well-described by our asymptotic expressions.

Acknowledgments

We are grateful to the members of the A(nisotropy)-Team of the Center for Wave Phenomena (CWP), Colorado School of Mines, for fruitful discussions. Colin Thomson (Schlumberger), Paul Martin (CSM), and Matthew Reynolds (CU Boulder) provided valuable help with asymptotic analysis and linear algebra. This work was supported by the Consortium Project on Seismic Inverse Methods for Complex Structures at CWP.

REFERENCES

- Aki, K., and P. G. Richards, 1980, *Quantitative Seismology: Theory and Methods*, Volume I: W.H. Freeman and Company.
- Behura, J., and I. Tsvankin, 2009, Role of the inhomogeneity angle in anisotropic attenuation analysis: *Geophysics*, **74**, no. 5, WB177–WB191.
- Bleistein, N., 1984, *Mathematical Methods for Wave Phenomena*: Academic Press.
- , 2012, Saddle point contribution for an n-fold complex-valued integral: CWP Research Report 741.
- Carcione, J., 2007, *Wave Fields in Real Media. Theory and numerical simulation of wave propagation in anisotropic, anelastic, porous and electromagnetic media.*: Elsevier.
- Červený, V., 1972, Seismic rays and ray intensities in inhomogeneous anisotropic media: *Geophysical Journal of the Royal Astronomical Society*, **29**.
- , 2001, *Seismic ray theory*: Cambridge University Press.
- Červený, V., L. Klimeš, and I. Pšenčík, 2008, Attenuation vector in heterogeneous, weakly dissipative, anisotropic media: *Geophysics Journal International*, **175**, 346–355.
- Červený, V., and I. Pšenčík, 2005, Plane waves in viscoelastic anisotropic media – I. Theory: *Geophysics Journal International*, **161**, 197–212.
- , 2008, Quality factor Q in dissipative anisotropic media: *Geophysics*, **73**, T63–T75.
- , 2009, Perturbation Hamiltonians in heterogeneous anisotropic weakly dissipative media: *Geophysics Journal International*, **178**, 939–949.
- Courant, R., 1988, *Differential and Integral Calculus*: Wiley-Interscience, **2**.
- Gajewski, D., 1993, Radiation from point sources in general anisotropic media: *Geophysics Journal International*, **113**, 299–317.
- Hearn, D. J., and E. S. Krebs, 1990, On computing ray-synthetic seismograms for anelastic media using complex rays: *Geophysics*, **55**, 422–432.
- Horn, R. A., and C. R. Johnson, 1990, *Matrix Analysis*: Cambridge University Press.
- Klimeš, L., 2002, Second-order and higher-order perturbations of travel time in isotropic and anisotropic media: *Studia Geophysica et Geodaetica*, **46**, 213–248.
- Krebs, E. S., and L. H. T. Le, 1994, Inhomogeneous plane waves and cylindrical waves in anisotropic anelastic media: *Journal of Geophysical Research*, **99**, 899–919.
- Tsvankin, I., 1995, *Seismic wavefields in layered isotropic media (course notes)*: Samizdat Press (<http://samizdat.mines.edu/>).
- , 2012, *Seismic signatures and analysis of reflection data in anisotropic media*, third ed.: Society of Exploration Geophysicists.
- Tsvankin, I., and V. Grechka, 2011, *Seismology of azimuthally anisotropic media and seismic fracture characterization*: SEG.
- Vavryčuk, V., 2007, Asymptotic Green’s function in homogeneous anisotropic viscoelastic media: *Proceedings of The Royal Astronomical Society*, **463**, 2689–2707.
- Wang, C. Y., and J. D. Achenbach, 1994, Elastodynamic fundamental solutions for anisotropic solids: *Geophysics Journal International*, **118**, 384–392.
- Zhu, Y., 2006, *Seismic wave propagation in attenuative anisotropic media*: PhD thesis, Colorado School of Mines.
- Zhu, Y., and I. Tsvankin, 2006, Plane-wave propagation in attenuative transversely isotropic media: *Geophysics*, **71**, no.2, T17–T30.

Appendix A

Exact Green's function for attenuative anisotropic media

The wave equation in the frequency-wavenumber domain for a homogeneous, attenuative, anisotropic medium can be written as (Zhu, 2006):

$$(\tilde{a}_{ijkl}(\omega)k_jk_l - \omega^2\delta_{ik})\tilde{U}_k(\mathbf{k}, \omega) = \tilde{f}_i(\mathbf{k}, \omega), \quad (23)$$

where ω is the frequency, \tilde{a}_{ijkl} are the components of the density-normalized stiffness tensor, k_j are the wavenumbers, $\tilde{\mathbf{U}}$ is the displacement vector, and $\tilde{f}(\mathbf{k}, \omega)$ is the body force per unit volume (source). All indices vary from 1 to 3.

The frequency-domain displacement can be found as the Fourier integral:

$$\tilde{u}_k(\mathbf{x}, \omega) = \frac{1}{(2\pi)^3} \int_{-\infty}^{\infty} \int_{-\infty}^{\infty} \int_{-\infty}^{\infty} \tilde{U}_k(k, \omega) e^{ik_j x_j} d\mathbf{k}, \quad (24)$$

where

$$\tilde{U}_k(k, \omega) = \frac{\tilde{B}_{ki} \tilde{f}_i(k_j, \omega)}{\det \tilde{\mathbf{D}}} \quad (25)$$

and $d\mathbf{k} = dk_1 dk_2 dk_3$. The matrix $\tilde{\mathbf{D}}$ ($\tilde{D}_{ki} = \tilde{a}_{ijkl}k_jk_l - \omega^2\delta_{ik}$) with cofactors \tilde{B}_{ki} is closely related to the Christoffel matrix. The source in equation 25 can be defined as a point impulsive force applied at location \mathbf{x}_0 parallel to the x_n -axis:

$$\tilde{f}_i(\omega, k_j) = \delta_{in} e^{-ik_j x_j^0}. \quad (26)$$

The particle displacement from this source is the Green's function:

$$G_{kn}(\mathbf{x}, \mathbf{x}^0, \omega) = \frac{1}{(2\pi)^3} \int_{-\infty}^{\infty} \int_{-\infty}^{\infty} \int_{-\infty}^{\infty} \frac{\tilde{B}_{ki} \delta_{in}}{\det \tilde{\mathbf{D}}} e^{ik_j(x_j - x_j^0)} d\mathbf{k}. \quad (27)$$

The integral over k_3 in equation 27 can be extended into the complex plane $\tilde{k}_3 = \text{Re } k_3 + i \text{Im } k_3$. The closed contour includes the real axis and a semicircle with an infinitely large radius in the upper half-plane. The integral can then be evaluated by the residue theorem (i.e., by computing the residues at the poles), as described in Aki and Richards (1980) and Tsvankin (1995). The poles correspond to the roots of the following equation for k_3 :

$$\det \tilde{\mathbf{D}} = \det[\tilde{a}_{ijkl}k_jk_l - \omega^2\delta_{ik}] = 0. \quad (28)$$

Equation 28 is a sixth-order polynomial in k_3 that can have at most six distinct roots that correspond to up- and downgoing P-, S₁- and S₂-waves.

In nonattenuative media, the roots of k_3 lie on the real k_3 -axis, and the integral can be evaluated by introducing small attenuation, moving the roots into the complex plane, and applying the residue theorem (Tsvankin, 1995). Alternatively, the integral over k_3 can be evaluated using Cauchy's principal value (Bleistein, 1984). In the presence of attenuation, the roots of equation 28 lie in the complex plane. The pole $\tilde{k}_3^r = \tilde{k}_3(k_1, k_2)$, which corresponds to a certain mode (e.g., P-waves) and is located inside the integration contour, yields the residue for that mode. The integral over k_3 in equation 24 reduces to the residue at the pole, and the Green's function becomes:

$$G_{kn}(\mathbf{x}, \mathbf{x}^0, \omega) = \frac{i}{(2\pi)^2} \int_{-\infty}^{\infty} \int_{-\infty}^{\infty} \left[\frac{\tilde{B}_{kn}}{\partial(\det \tilde{\mathbf{D}})/\partial k_3} \right]_{k_3=\tilde{k}_3^r} \times e^{i[k_1(x_1-x_1^0)+k_2(x_2-x_2^0)+\tilde{k}_3^r(x_3-x_3^0)]} dk_1 dk_2. \quad (29)$$

Substituting $k_j = \omega p_j$, where p_j denotes the components of the slowness vector, yields $\det \tilde{\mathbf{D}} = \omega^6 \det(\tilde{\Gamma}_{ik} - \delta_{ik})$, where $\tilde{\Gamma}_{ik} = a_{ijkl}p_jp_l$. The cofactors of $\tilde{\Gamma} - \mathbf{I}$ (\mathbf{I} is the identity matrix) are denoted by S_{kn} , and $B_{kn} = \omega^4 S_{kn}$. Equation 29 can then be written as

$$G_{kn}(\mathbf{x}, \mathbf{x}^0, \omega) = \frac{i\omega}{(2\pi)^2} \int_{-\infty}^{\infty} \int_{-\infty}^{\infty} \left[\frac{\tilde{S}_{kn}}{\partial[\det(\tilde{\Gamma} - \mathbf{I})]/\partial p_3} \right]_{p_3=\tilde{p}_3^r} \times e^{i[p_1(x_1-x_1^0)+p_2(x_2-x_2^0)+\tilde{p}_3^r(x_3-x_3^0)]} dp_1 dp_2. \quad (30)$$

Appendix B**Perturbation analysis for anisotropic attenuative media**

In this section, we present approximate expressions for the propagation and attenuation vectors (and, hence, the inhomogeneity angle) in homogeneous, attenuative, anisotropic media using the method of perturbation Hamiltonians introduced by Červený and Pšenčík (2009). We also derive the conditions under which the inhomogeneity angle vanishes.

In their methodology, Červený and Pšenčík (2009) treat the traveltime as a complex-valued quantity, with the real part contributing to the phase and the imaginary part to the dissipation along the ray. The complex-valued traveltime and traveltime gradients can be computed as a perturbation of the corresponding real-valued quantities found along the ray. The density-normalized stiffness tensor is given by $\tilde{a}_{ijkl} = a_{ijkl}^R - i a_{ijkl}^I$, with the real part corresponding to the reference nonattenuative medium, and the imaginary part to the perturbation that makes the medium viscoelastic.

We consider the linear perturbation Hamiltonian $\mathcal{H}(\mathbf{x}, \mathbf{p}, \alpha)$ defined in Červený and Pšenčík (2009):

$$\mathcal{H}(\mathbf{x}, \mathbf{p}, \alpha) = \mathcal{H}^0(\mathbf{x}, \mathbf{p}) + \alpha \Delta \mathcal{H}(\mathbf{x}, \mathbf{p}), \quad (1)$$

with

$$\Delta \mathcal{H}(\mathbf{x}, \mathbf{p}) = \tilde{\mathcal{H}}(\mathbf{x}, \mathbf{p}) - \mathcal{H}^0(\mathbf{x}, \mathbf{p}), \quad (2)$$

where \mathcal{H}^0 and $\tilde{\mathcal{H}}$ correspond to the (elastic) reference and (viscoelastic) perturbed medium, respectively, \mathbf{p} is the slowness vector, and α is the perturbation parameter. The reference Hamiltonian \mathcal{H}^0 can be expressed through the slowness (\mathbf{p}) and polarization (\mathbf{g}) vectors computed for the reference medium:

$$\mathcal{H}^0(\mathbf{x}, \mathbf{p}) = \frac{1}{N} [a_{ijkl}^R p_j p_l g_i g_k]^{N/2}, \quad (3)$$

where N is an integer. The polarization vector \mathbf{g} satisfies the equation

$$\Gamma_{ik} g_k = [a_{ijkl}^R p_j p_l] g_k = \lambda g_i, \quad (4)$$

where λ represents the eigenvalue of the Christoffel matrix for the mode of interest. The perturbed Hamiltonian $\tilde{\mathcal{H}}$ is given by

$$\tilde{\mathcal{H}}(x_m, p_n) = \frac{1}{N} [\tilde{a}_{ijkl} p_j p_l \tilde{g}_i \tilde{g}_k]^{N/2}, \quad (5)$$

where the complex polarization vector $\tilde{\mathbf{g}}$ is computed as the eigenvector of the complex Christoffel matrix $\tilde{\Gamma}_{ik}$:

$$\tilde{\Gamma}_{ik} \tilde{g}_k = [\tilde{a}_{ijkl} p_j p_l] \tilde{g}_k = (\lambda + \Delta \lambda) g_i, \quad (6)$$

where λ is the eigenvalue that corresponds to the reference elastic medium and $\Delta \lambda$ is the perturbation of λ . The slowness vector \mathbf{p} in equations 5 – 6 corresponds to the reference elastic medium and is real-valued.

The traveltime gradient, which corresponds to the perturbation Hamiltonian defined in equation 5, can be expanded in the perturbation parameter α (Červený and Pšenčík, 2009):

$$\frac{\partial \tau}{\partial x_i} \approx \frac{\partial \tau^0}{\partial x_i} + \alpha \left[\frac{\partial^2 \tau}{\partial x_i \partial \alpha} \right]_{\alpha=0} + \dots, \quad (7)$$

where $\partial \tau^0 / \partial x_i = p_i^0$ is computed in the reference medium. An approximation for the the traveltime gradient in attenuative media can be obtained by substituting $\alpha = 1$ and retaining the first two terms of the expansion in equation 7. Then the real part of the traveltime gradient corresponds to \mathbf{p}^R and the imaginary part to \mathbf{p}^I :

$$p_i^R = \text{Re} \left[\frac{\partial \tau}{\partial x_i} \right] \approx p_i^0 + \text{Re} \left[\frac{\partial^2 \tau}{\partial x_i \partial \alpha} \right]_{\alpha=0}, \quad (8)$$

$$p_i^I = \text{Im} \left[\frac{\partial \tau}{\partial x_i} \right] \approx \text{Im} \left[\frac{\partial^2 \tau}{\partial x_i \partial \alpha} \right]_{\alpha=0}. \quad (9)$$

The inhomogeneity angle can be computed from

$$\cos \xi = \frac{\mathbf{p}^I \cdot \mathbf{p}^R}{|\mathbf{p}^I| |\mathbf{p}^R|}. \quad (10)$$

The second-order partial derivative in equation 7 is evaluated using quadratures along the reference rays. Detailed derivations and the methodology can be found in Klimeš (2002) and Červený and Pšenčík (2009). Here, we will only

provide the expressions corresponding to the perturbation Hamiltonian defined in equation 1 for a homogeneous medium. The relevant expressions are

$$\frac{\partial^2 \tau}{\partial x_i \partial \alpha} = \tilde{T}_k(\alpha) [Q_{ki}^{\text{ray}}]^{-1}, \quad (11)$$

with the vector $T_k(\alpha)$ given by

$$\tilde{T}_K(\alpha) = \tilde{T}_K^0(\alpha) + \tau \tilde{W}_i P_{iK}^{\text{ray}}, \quad K = 1, 2, \quad (12)$$

$$\tilde{W}_i = \left(\frac{\partial \tilde{\mathcal{H}}}{\partial p_i} - \frac{\partial \mathcal{H}^0}{\partial p_i} \right), \quad (13)$$

$$\tilde{T}_3(\alpha) = \mathcal{H}^0 - \tilde{\mathcal{H}}. \quad (14)$$

The upper-case index “ K ” changes from 1 to 2, and the lower-case index “ k ” from 1 to 3. The real-valued matrices Q_{ik}^{ray} (not to be confused with the quality-factor matrix) and P_{ik}^{ray} are computed during dynamic ray tracing in the reference elastic medium. They are defined as:

$$\begin{aligned} Q_{ik}^{\text{ray}} &= \frac{\partial x_i}{\partial \gamma_k}, \\ P_{ik}^{\text{ray}} &= \frac{\partial p_i^0}{\partial \gamma_k}; \end{aligned} \quad (15)$$

γ_k denotes a certain “ray parameter” (e.g. the initial phase angle or the traveltime along the ray). In equation 12, $\tilde{T}_K^0(\alpha) = 0$ for a point source, however, for plane-wave propagation the values of $\tilde{T}_K^0(\alpha)$ (initial conditions) may be chosen arbitrarily (Klimeš, 2002).

We now derive the conditions under which the inhomogeneity angle vanishes in homogeneous media. Substituting equations 3 and 5 into equation 13 yields:

$$\tilde{W}_i = \tilde{a}_{ijkl} p_k \tilde{g}_j \tilde{g}_l - a_{ijkl}^R p_k g_j g_l. \quad (16)$$

For weakly dissipative media, we can use the approximation $\tilde{\mathbf{g}} \approx \mathbf{g}$ and reduce equation 16 to

$$\tilde{W}_i = -i a_{ijkl}^I p_k g_j g_l. \quad (17)$$

For the special case of identical Q components (i.e., $a_{ijkl}^I = a_{ijkl}^R/Q$), we have

$$\tilde{W}_i = -i \frac{a_{ijkl}^R}{Q} p_k g_j g_l = -i \frac{\mathcal{U}_i}{Q}, \quad (18)$$

where \mathcal{U}_i are the components of the group-velocity vector in the reference elastic medium. Substituting equation 18 into equation 12, we obtain

$$\tilde{T}_{K\alpha}(\gamma_3) = -i(\gamma_3 - \gamma_3^0) \frac{\mathcal{U}_i}{Q} P_{iK}^{\text{ray}} = 0, \quad K = 1, 2, \quad (19)$$

because the group-velocity vector is orthogonal to the first two columns of the matrix \mathbf{P}^{ray} , i.e., $\mathcal{U}_i P_{iK} = 0$ (Červený, 2001). Then, equations 8 and 9 for \mathbf{p}^R and \mathbf{p}^I take the form:

$$p_i^R = p_i^0 + \text{Re} [\tilde{T}_{3\alpha}] p_i^0, \quad (20)$$

and

$$p_i^I = \text{Im} [\tilde{T}_{3\alpha}] p_i^0, \quad (21)$$

where $p_i^0 = [Q_{3i}^{\text{ray}}]^{-1}$ (Červený, 2001). From equations 20 and 21, it follows that \mathbf{p}^R is parallel to \mathbf{p}^I . Hence, the inhomogeneity angle vanishes in the case of identical Q components, i.e., when the attenuation coefficients of all three wave-modes are isotropic. Note that the velocity function may still be anisotropic. Further, the inhomogeneity angle also vanishes for isotropic velocity and attenuation functions. This can be proved by substituting the expressions for the Hamiltonian in isotropic media into equation 16.

